Temperature Dependence of CO Oxidation on Rh(111) by Adsorbed Oxygen

Marie E. Turano, Rachael G. Farber[†], George Hildebrandt, and Daniel R. Killelea*

Department of Chemistry & Biochemistry, Loyola University Chicago, 1068 W. Sheridan Rd., Chicago IL 60660

Revised submission to *Surface Science*

*Corresponding Author. Email address: dkillelea@luc.edu; ph: (773) 508 - 3136

[†]Present address: James Franck Institute and Department of Chemistry, The University of Chicago, Chicago, IL 60637

Abstract

Carbon monoxide oxidation over oxidized Rh surfaces is known to be sensitive to both the oxygen species present as well as the surface temperature. Although CO oxidation on Rh(111) is a prototypical heterogeneously catalyzed oxidation reaction, questions remain about the reactivity of the individual oxygenaceous phases present on the surface. For example, the effects of surface temperature or the duration of CO exposure have not been previously determined on the oxygen-rich, (2×1)-O surface adlayer. In this paper, we present results from a study that used a combination of ultra-high vacuum surface science techniques to measure the oxidation of CO by oxygen in the (2×1)-O adlayer. The surface temperature during the CO exposure was varied between 100 K and 350 K, and the effect of the surface temperature on CO oxidation was determined for CO exposures between 5 L and 300 L. We observed that the surface temperature had little effect on the CO_2 yield or the amount of residual oxygen for CO exposures up to 300 K, but these quantities were reduced after CO exposures above 300 K. We also found that CO oxidation was unchanged by the extent of the CO exposure at both 300 K and 350 K. Taken together, these results show that CO was oxidized over the (2×1)-O adlayer during CO exposures above 300 K via a different reaction pathway than the one followed by co-adsorbed O and CO in the (2×2)-2O+CO adlayer and that these lower-barrier reactive sites were not regenerated during the CO exposure.

Keywords

Rhodium; CO Oxidation; adsorbed oxygen; catalysis

Introduction

Rhodium metal surfaces play key roles in important heterogeneously catalyzed reaction schemes such as the partial oxidation of methane, which is an effective approach to the generation of syngas [1-4]. Reactions on rhodium surfaces have attracted significant attention over the years because of rhodium's catalytic utility and its use in model systems to investigate surface-mediated oxidation reactions. Of particular interest were investigations of CO oxidation by different oxygen species on Rh surfaces, including adsorbed oxygen atoms (O_{ad}), the bulk oxide (Rh_2O_3), and the surface oxide (RhO_2)[5-10]. Recent work from our group has investigated the structural consequences of extensive oxidation of Rh(111) by gas-phase atomic oxygen (AO) which resulted in the formation of the (2×1)-O adlayer, subsurface oxygen (O_{sub}), and surface oxide phases. Additionally, it was shown that exposure of highly oxidized Rh(111) to CO at modest sample exposure temperatures (T_{exp}) resulted in CO oxidation at defect sites, such as domain boundaries, that removed nearly all the oxygen from the Rh(111) during the exposure, leaving little residual oxygen (O_{res}) [11-14]. Motivated by these results, we determined the reactivity of the (2×1)-O adlayer to better understand the enhanced reactivity when several phases co-exist.

O_2 readily dissociates into two O_{ad} on Rh(111). As the O coverage (θ_O) increases, the O atoms first arrange into a (2×2)-O adlayer with θ_O = 0.25 monolayers (ML, 1 ML = 1.6×10^{15} O_{ad} cm^{-2}). As more O sticks, θ_O increases to 0.5 ML, and the (2×2)-O adlayer transforms into a (2×1)-O adlayer [5, 15-19]. Further exposure to O_2 does not increase θ_O under low-pressure conditions because O_2 dissociation requires two adjacent vacant surface sites, which becomes increasingly unlikely as θ_O approaches 0.5 ML [20-22]. STM

images of Rh(111) with $\theta_O \approx 0.5$ ML clearly showed the surface was comprised of three different orientation of the (2×1)-O adlayer, each rotated by 120° with respect to each other; because of this, LEED analysis showed a (2×2) pattern [20, 23]. Although $\theta_O > 0.5$ ML is not achievable using low pressures of O_2, the use of more aggressive oxidants (e.g. NO_2, ozone, or AO) overcomes the kinetic limitations of O_2 dissociation and achieves significantly higher oxygen incorporation [13, 19, 20].

CO has a high sticking probability on Rh(111), and forms a (√3×√3)-R30° adlayer on Rh(111)[24, 25] with $\theta_{CO} \approx 1/3$ ML and prolonged CO exposures lead to higher CO coverages [26, 27]. On the (2×1)-O Rh(111) surface, CO molecules insert themselves as adsorbed CO (CO_{ad}) into the O adlayer, forming a (2×2)-2O+CO adlayer[17, 28, 29]. Between 350 K and 600 K, CO_{ad} is effectively oxidized by O_{ad} to form CO_2 (*g*), leaving behind approximately 0.25 ML O, but no CO_{ad}[7, 11, 30]. CO is also oxidized by the (9×9)-O surface reconstruction[31], the RhO_2 surface oxide[32], and other oxygen surface phases [11, 33, 34]. Although the overall kinetics of CO oxidation on rhodium have been investigated[7], it is unclear what the effects of T_{exp} and CO exposure on CO oxidation may be. This information is needed to better describe the temperature dependent reactivity of the (2×1)-O surface. In this paper, we present results from a study of CO oxidation where the extent of CO exposure and surface temperature of Rh(111) with an (2×1)-O adlayer were varied. We found that the amount of CO oxidized was largely insensitive to the duration of the CO exposures and the exposure temperature only had a modest effect. These results show that CO oxidation may occur via lower-barrier pathways, but co-adsorbed O and CO in the (2×2)-2O+CO adlayer remained inert and did not produce CO_2

at an appreciable rate up to 350 K. The reactive species or sites that oxidized CO at 350 K or below were not regenerated after they reacted to form CO_2.

Experimental

Experiments were conducted under UHV conditions. The interconnected UHV-STM system was previously described[14] and consists of two chambers: a preparatory/analysis chamber (base pressure of 1×10^{-10} torr) and a STM chamber (base pressure of 4×10^{-11} torr). The preparatory chamber was equipped with a PHI 10-155 Auger Electron Spectrometer (AES), a Fissions RVL900 low energy electron diffractometer (LEED), and a Hiden HAL 3F 301 RC quadrupole mass spectrometer (QMS) which was equipped with a shroud (also known as a Feulner cap[35]) to provide greater signal-to-noise during TPD measurements. The QMS was mounted on a translation stage, and was moved to within 3-4 mm of the front face of the Rh(111) crystal for TPD experiments.

The Rh(111) crystal (Surface Preparation Labs, Zaandam, The Netherlands) was mounted on an exchangeable tantalum (Ta) sample plate by welding to two supporting Ta wires underneath, and a type K thermocouple was welded directly to the back of the crystal for accurate temperature reading. The crystal could be cooled with a liquid nitrogen cooling loop to 100 K and heated using electron beam heating to 1400 K. The crystal was cleaned using the standard preparation cycles of Ar^+ sputtering followed by annealing at 1300 K. A 1300 K anneal was sufficient to clean the crystal between experiments. Surface cleanliness was verified with AES and a crisp (1×1) LEED pattern.

The (2×1)-O adlayer on Rh(111) was prepared by exposure to O_2 via backfilling the chamber to a pressure of 1×10^{-6} Torr for 60 seconds, equating to a 60 Langmuir (L, 1

L = 10^{-6} Torr s O_2) O_2 exposure. As demonstrated in previous publications, the coverage was determined to be 0.5 ML using a combination of LEED, AES, and STM [13, 14]. For CO exposures, the chamber was similarly backfilled to a pressure of 1×10^{-6} Torr for varying lengths of time while the Rh(111) crystal was held at T_{exp}. Two sequential TPDs were then performed: one from 100 K to 600 K with a ramp rate of 4 K s^{-1} for CO and CO_2 desorption (CO_2 yield) , and one from 400 K to 1400 K with a ramp rate of 3 K s^{-1} for recombinative desorption of residual O (O_{res}) as O_2. The STM was a PanScan Freedom STM from RHK Technology, cooled by a closed-cycle He cryostat, and a temperature of 30 K was used for imaging. A cut and pull 80% Pt, 20% Ir 0.25 mm diameter wire was used as the tip. All images were recorded in constant current mode. No drift correction was applied to the images, but limited processing (e.g. cropping, mean-plane subtraction, or removal of streaks or blemishes) was performed using the Gwyddion[36] software package (available at http://gwyddion.net).

Results and Discussion

The (2×1)-O Rh(111) surface was exposed to 30 L carbon monoxide (CO) at various temperatures (T_{exp}). During a TPD measurement between 100 K and 600 K, CO_{ad} was oxidized to form CO_2, as shown in Figure 1A. The CO_2 yield (Y_{CO_2}) showed only slight variations as a function of T_{exp} between 100 K and 350 K. The CO_2 reaction product desorbed in a broad feature between 350 K and 550 K, and the peak shape changed slightly as T_{exp} was increased from 200 K to 350 K; but for all T_{exp} conditions, neither dramatic changes in the shape of the desorption peak nor its intensity were observed. However, the changes in the CO_2 desorption are worth noting, because the different desorption peaks suggest different reaction pathways. For T_{exp} < 300 K, the CO_2 desorption trace had two

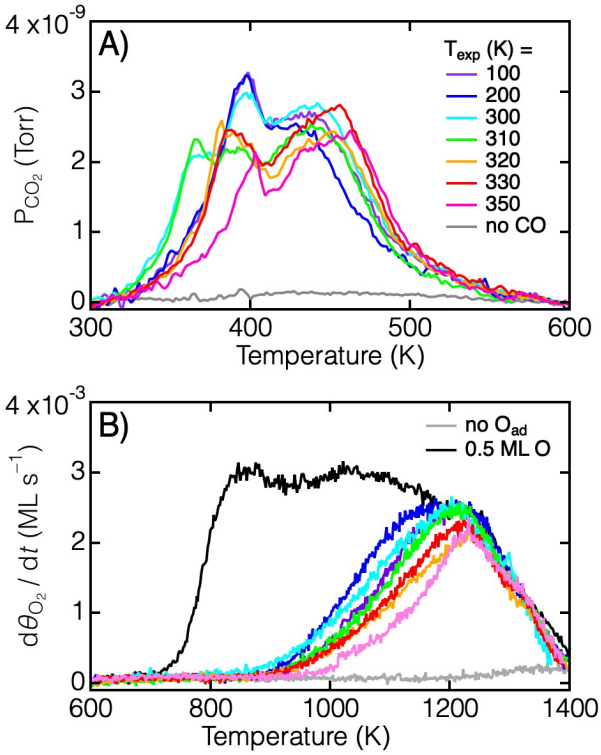

Figure 1: TPD spectra after exposure of 30 L CO at various temperatures (T_{exp}) to 0.5 ML O on Rh(111) in (2×1)-O adlayer. A) CO_2 desorption from the reaction between O_{ad} and CO_{ad} during TPD ramp to 600 K. B) TPD of residual oxygen after $O_{ad} + CO_{ad} \rightarrow CO_2$ (*g*) reaction.

peaks, one near 400 K, and a broader peak near 450 K. For T_{exp} = 300 K, a lower-temperature shoulder was observed around 375 K. With increasing T_{exp}, the shoulder and 400 K desorption peak blended together, and slightly decreased in intensity, until, for T_{exp} = 350 K, the shoulder was gone and the 400 K peak was significantly attenuated. Such behaviors were not surprising because the CO oxidation rate was appreciable at 350 K, as indicated in the CO_2 TPD experiment in Figure 1A. The shoulder and two peaks in the CO_2 desorption spectra were indicative of different CO oxidation mechanisms or sites, because the higher temperature desorption peak was far less sensitive to T_{exp} than the lower temperature desorption features. At the same time, the higher temperature peak broadened further and shifted to higher temperature, possibly because the reaction was occurring on

a more ordered surface that required additional thermal energy to overcome the reaction (or diffusion) barriers.

To better understand the TPD data, LEEDs were taken after 30 L CO exposures at T_{exp} = 300 K and T_{exp} = 350 K, as well as after the CO_2 TPD, as shown in Figure 2. These two temperatures represent the regimes under which distinctly different CO_2 and O_{res} desorption quantities were observed. Following exposure of Rh(111) with the (2×1)-O adlayer to 30 L CO at either T_{exp} = 300 K or 350 K, the LEED showed a (2×2) pattern (Figures 2A and 2C). These LEED patterns were in agreement with other studies after similar exposures of CO on 30 L O_2 on Rh(111)[37] and show the extensive formation of the (2×2)-2O+CO adlayer. The surface was likely more ordered after CO exposure at 350 K than 300 K, as the LEED pattern for T_{exp} = 350 K was a bit sharper than the one from the 300 K CO exposure. However, the same pattern was observed for both exposure temperatures.

Figure 1B shows the recombinative desorption of residual oxygen (O_{res}) during a TPD measurement from 600 K to 1400 K. These spectra quantified the coverage of O_{res} ($\theta_{O,\,res}$) adsorbed to the Rh(111) surface after CO_{ad} was oxidized or desorbed. The black trace in Figure 1B corresponds to the θ_O = 0.5 ML (2×1)-O surface with no CO exposure, and was used as a benchmark to quantify $\theta_{O,\,res}$ on Rh(111) [14]. If there was no O_{res}, then this indicated that O_{ad} was the limiting reagent and would have been entirely consumed by some combination of oxidation of impinging CO during the CO exposure and/or subsequent reaction with CO_{ad} during the TPD measurement. Compared to the pristine (2×1)-O TPD, it was clear that although a 30 L CO exposure caused a sizable decrease in O_{res} at all temperatures, $\theta_{O,\,res} > 0$ for all conditions. After an abrupt change at T_{exp} = 300

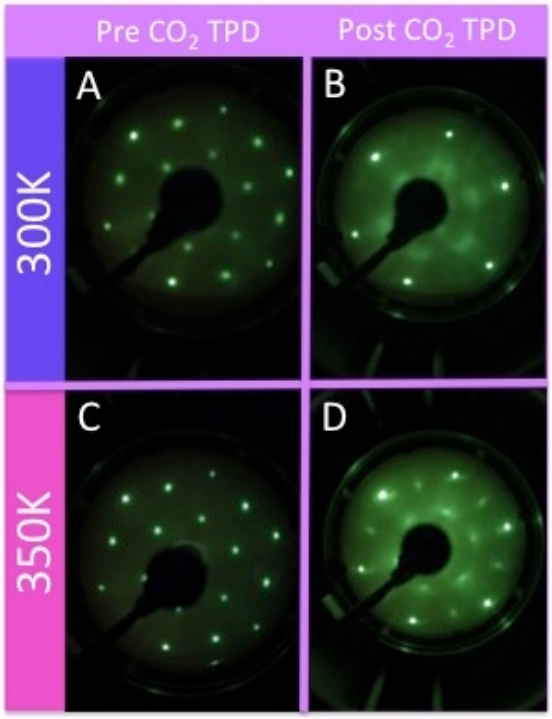

Figure 2: LEED patterns taken of (2×2)-2O+CO on Rh(111) after 30 L CO exposures at A) 300 K and C) 350 K. The LEED patterns shown in B) and D) are from the residual oxygen remaining after heating the surfaces to 600 K in a TPD experiment to oxidize and desorb CO_{ad}. All LEED patterns were taken with an electron energy of 62 eV.

K, there was only a modest decrease in $\theta_{O,\,res}$ with increasing T_{exp}. Each iteration of the experiment began with the same (2×1)-O θ_O = 0.5 ML surface, so the initial θ_O was the same for all doses; any observed decrease in residual oxygen would have been the result of either reaction with CO adsorbed to the O-covered, or oxidation of CO to CO_2 during the CO exposure.

Figure 3 shows the coverage of residual oxygen ($\theta_{O,\,res}$, left axis, in red) and the desorption of CO_2 (right axis, in blue) plotted against CO exposure temperature (T_{exp}). For T_{exp} between 100 K and 300 K, Y_{CO_2} decreased slightly, but $\theta_{O,res}$ was essentially unchanged. This suggests that a bit more CO may adsorb at lower T_{exp}, slightly enhancing the oxidation of CO to CO_2. For T_{exp} > 300 K, there was an abrupt decrease in $\theta_{O,res}$ and a

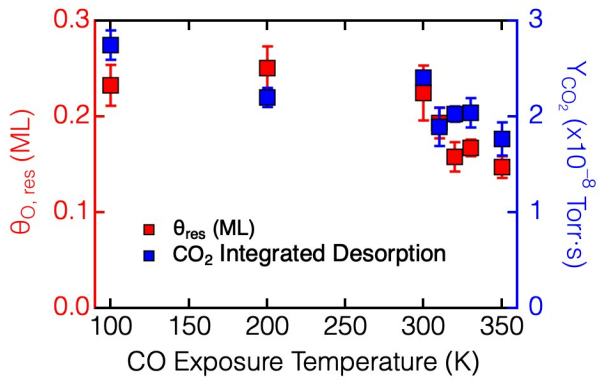

Figure 3: Coverage of residual oxygen ($\theta_{O,\,res}$, left axis) and CO_2 yield (Y_{CO_2}, right axis) plotted against the CO exposure temperature. The data points are the average integrals of the TPD spectra, error bars indicate 95% confidence interval. Representative spectra are shown in Figure 1.

slight decrease in Y_{CO_2}. However, further increase in T_{exp} had little effect on the amount of CO_2 that desorbed. Now, because the sample was cooled to below 100 K after the CO exposure, a significant amount of time elapsed between the CO exposure and the TPD measurement. Therefore, because the CO_2 yield observed in the TPD experiment did not vary depending on the time elapsed between the start of the dose and TPD measurement, other reactions, e.g. reactions with background gases or slower regeneration of more reactive sites, were not removing O_{ad} or CO_{ad}. Therefore, the CO_2 observed in the TPD experiment could only have been from the Langmuir-Hinshelwood reaction between O_{ad} and CO_{ad}. Previous work have demonstrated that O_{ad} was more tightly bound to Rh(111) that CO_{ad} and O_{ad} prefer different surface sites with CO_{ad} at fcc top sites[37, 38] and O_{ad} on bridge sites[38]. Because the two adsorbates preferred different binding sites, O_{ad} does not hinder CO adsorption[33]. Additionally, the barrier for CO diffusion is significantly lower than for desorption [7, 30, 38, 39], implying that co-adsorbed CO and O remained until reaction occurred. Therefore, when $\theta_{O,\,res} > 0$, CO was the limiting reagent and Y_{CO_2} was representative of the amount of CO adsorbed to the surface. It is apparent from Figures 1 and 3, that the amount of CO_{ad} was modestly more for $T_{exp} < 300$ K, dropped for $T_{exp} >$

300 K, and then was largely unaffected when T_{exp} was between 300 K and 350 K. An additional point is that the indicator for CO oxidation during the CO exposure is not Y_{CO_2}, but would be $\theta_{O,res}$; the oxygen remaining on the Rh(111) surface after CO_{ad} was removed by oxidation or desorption.

$\theta_{O,res}$ is shown by the red data points in Figure 3. It is clear that there was a significant decrease in $\theta_{O,res}$ going from T_{exp} = 300 K to 310 K. As T_{exp} was further increased to 350 K, there was a roughly linear decrease of $\theta_{O,res}$ with increasing CO exposure temperature, but the magnitude of decrease was smaller than the initial step from 300 K to 310 K. In the temperature regime 300 K < T_{exp} ≤ 350 K, Y_{CO_2} was flat, as discussed above, suggesting the amount of CO_{ad} was roughly constant. However, the decrease in $\theta_{O,res}$ meant that some CO was oxidized during the exposure, decreasing θ_O. Again, this was anticipated based on the TPD data. Because O_{ad} was not completely removed, the reaction probability must have dropped as the CO exposure continued.

The changes in the surface structure after the CO_2 TPD are shown by the LEED patterns in Figure 2B and 2D, and it is clear that T_{exp} had a significant effect on the resultant surfaces. For CO exposure at T_{exp} = 300 K (Figure 2B), the (2×2) pattern was eliminated and a new pattern consisting of (1×1) spots, a hazy center pattern reminiscent of a flower, and faint, diffuse spots in the half-order position between the (1×1) spots was observed. The presence of these diffuse spots after oxidation suggests that reaction disrupts the surface order and increased temperatures were not sufficient to restore the surface. O_{res} were largely stochastically distributed about the surface and were not in islands of either the (2×2)-O or (2×1)-O adlayer. Alternatively, the LEED pattern for O_{res} from CO

exposure at T_{exp} = 350 K (Figure 2D) retained the (2×2) pattern, although the half-order spots were rather distorted. From the data in Figure 3, $\theta_{O,res} \approx 0.25$ ML for T_{exp} = 300 K. $\theta_{O,res}$ dropped to ≈ 0.15 ML for T_{exp} = 350 K, indicating a 40 % decrease in $\theta_{O,res}$. The

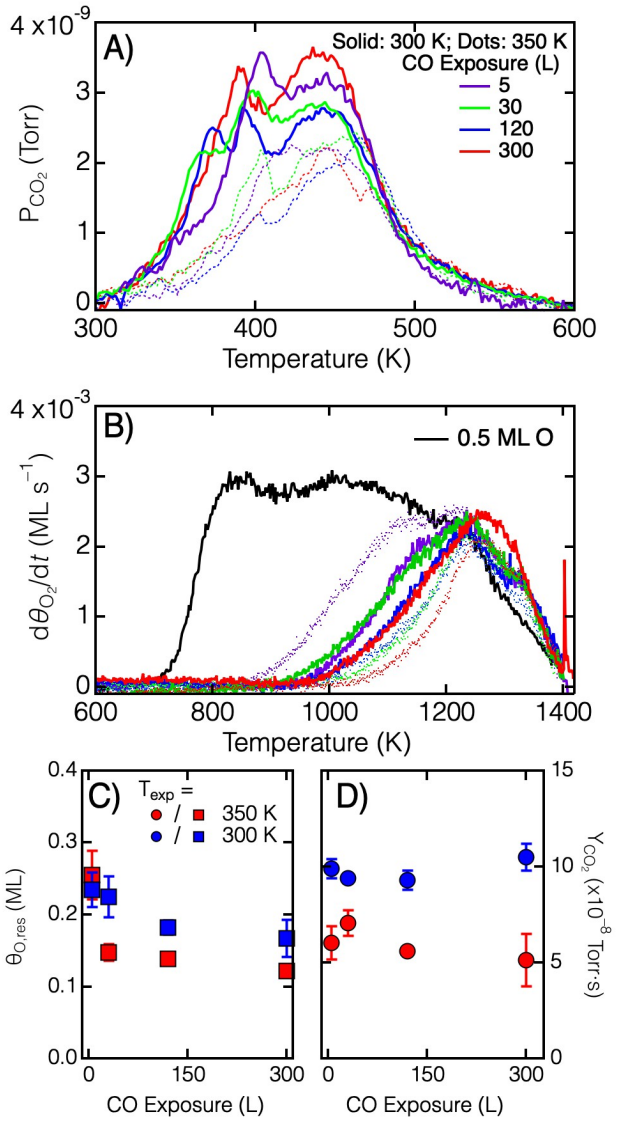

Figure 4: CO_2 yield (Y_{CO_2}2) and residual O_{ad} for varying CO exposure at 350 K and 300 K. A) TPDs showing the CO_2 desorption for CO exposures of 5 L, 30 L, 120 L, and 300 L. B) TPDs showing the desorption of the residual O_{ad} after reaction with CO_{ad}. In both A) and B) the solids lines correspond to CO exposures at 300 K and the dotted at 350 K. The colors correspond to the same CO exposures in both. C) and D) show the residual oxygen coverage ($\theta_{O,res}$) and Y_{CO_2}, respectively. For CO exposure at 300 K, there is little change in either $\theta_{O,res}$ or Y_{CO_2} after 30 L CO. At 350 K, Y_{CO_2} was also insensitive to CO exposure, but $\theta_{O,res}$ shows a small decrease going from 30 L to 120 L CO.

remaining O_{res} were likely arranged in a (2×2)-O adlayer with sizable areas of randomly distributed chemisorbed O atoms, as θ_O was less than the 0.25 ML O required to cover the entire surface in the (2×2)-O adlayer. There was also a 30 % decrease in Y_{CO_2} comparing T_{exp} 300 K to 350 K. The fact that both $\theta_{O,res}$ and Y_{CO_2} decreased meant that there was less CO adsorbed to the surface after exposure, and the CO reacted away more O_{ad} at 350 K than at 300 K. However, there was still ample O_{res}, meaning that the reaction pathway enhanced at 350 K, when compared to 300 K, was not accessible everywhere on the surface and that the reactive surface sites or species were not regenerated during the CO exposure.

The relatively modest impact of variation in the surface temperature of the (2×1)-O adlayer on Rh(111) during exposure to CO was likely the result of oxidation at surface sites the offered lower barrier reaction pathways, but it is unclear if such sites would be restored to further oxidize CO, for all the experiments discussed above were for CO exposures of the same 30 L duration. Because the rate of CO_2 formation was appreciable at 350 K (as shown by the above-baseline partial pressure of CO_2 in Figure 1A), it is plausible to assume that if the sites were regenerated at 350 K, prolonged CO exposure times would have continued to remove O_{ad} as the CO exposure progressed. Conversely, if such sites were not regenerated and CO simply stuck to the surface forming the (2×2)-2O+CO adlayer, both $\theta_{O,res}$ and Y_{CO_2} would be invariant with CO exposure. As we show below, the latter case was observed, indicating that CO oxidation proceeds via different pathways on the (2×1)-O adlayer on Rh(111). The existence of different reaction mechanisms at different surface sites has recently been observed for CO oxidation on the steps and terraces of platinum, where Neugebohren *et al*. found that the lowest-barrier

reaction pathway was between O_{ad} on steps and rapidly diffusing CO from the terraces [40]. It is possible that Rh behaves similarly.

Figure 4 shows TPDs of CO_2 desorption (Figure 4A), as well as the desorption of O_{res} (Figure 4B) for several CO exposures at both 300 K and 350 K. Figures 4C and 4D show plots of $\theta_{O,res}$ and Y_{CO_2} vs. CO exposure, respectively. It is clear from Figure 4 that increased CO exposures over 5 L had, at most, a modest effect on $\theta_{O,res}$ or Y_{CO_2} for CO exposures at either 300 K (blue data points) or 350 K (red data points). This implies that the 5 L CO exposure was sufficient to cover the surface in the (2×2)-2O+CO adlayer and that CO_2 desorption between 350 K and 550 K was from that phase as well. For CO exposures at 300 K, there was consistently more CO_2 and O_{res} than for the 350 K exposures, again suggesting that some O_{ad} was reacted away during the CO exposure at 350 K. However, prolonged CO exposures at either 300 K or 350 K did not further diminish $\theta_{O,res}$ suggesting that whatever species or sites that were responsible for the oxidation reaction were consumed by CO exposures of 5 L or less and were not regenerated. This was in marked contrast to our previous observation of a strong dependence of O_{res} on CO exposure for the mixed (2×1)-O and RhO_2 oxide with O_{sub}, where O was nearly entirely consumed during the 300 K CO exposure, leaving only a small amount of O_{ad} in the (2×2)-2O+CO adlayer[11]. Although the reaction rate is non-zero for CO_2 formation at 350 K (as shown by the TPDs in Figures 1 and 4), the reaction that manifests itself as the shoulder and 400 K CO_2 desorption peak has run its course by the time the T_{exp} = 350 K CO exposure reached 30 L. After the reactions occurred, these lower barrier sites were inert and could only adsorb CO that was not oxidized later, as the area would be denuded of O_{ad}. Unfortunately, we were unable to detect desorption of CO_{ad} reliably and quantitatively during the TPD

measurement because of the significant background of CO and the cracking of CO_2 in the QMS ionizer.

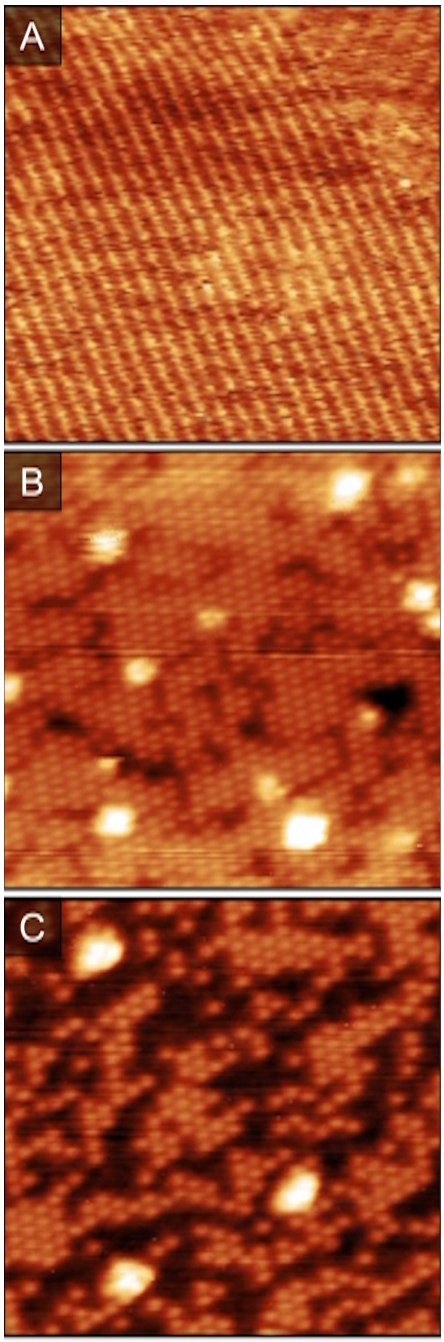

Figure 5: 15 × 15 nm^2 STM images of: A) the (2×1)-O adlayer after a 60 L O_2 exposure at 300 K; B) the (2×2)-2O+CO after a 2 L CO exposure at 220 K; and C) the (2×2)-2O+CO adlayer in B) after annealing at 325 K. Imaging conditions were A) -108 mV, -0.61 nA; B) 0.84 V, 180 pA; C) 0.69 V, 256 pA.

In order to investigate how the surface changed as the temperature was raised above 300 K, we obtained STM images of the surface before and after annealing at 325 K, a low enough temperature where we would not expect an appreciable amount of CO oxidation. Figure 5A shows an STM image of Rh(111) after an exposure of 60 L O_2 at 300 K resulting in a complete (2×1)-O adlayer. The (2×1)-O adlayer has been previously described [14, 16, 23] and the co-existence of different domains rotated by 120° were evident in the upper right corner of Figure 5A. Following a 2 L CO exposure at 220 K, the surface was predominantly covered in the (2×2)-2O+CO adlayer, as shown in Figure 4B. The bright circular features in the (2×2)-2O+CO structure were adsorbed CO molecules. The bright white blotches were likely spurious adsorbed species or CO. Upon annealing this surface at 325 K, the surface changed slightly, as shown in Figure 5C. The occurrence of bright raised areas decreased, and there were more dark regions between areas of (2×2)-2O+CO. The result was that the (2×2)-2O+CO structure was still predominant, but its coverage decreased slightly compared to the unannealed (2×2)-2O+CO surface. It is important to note that the STM images were taken after brief CO exposures where the surface would not be fully covered in the (2×2)-2O+CO adlayer; such coverage would not be expected until an exposure of closer to 30 L CO. Despite not having a full adlayer, the apparent CO coverage still decreased between Figures 5B and 5C. The CO molecules remained in the (2×2) registry and were aligned with the (2×1)-O adlayer, indicating that CO was not oxidized on the surface, but more likely desorbed as intact CO. We were unable to determine the surface structure in the dark regions of the STM images, but assume they are (2×1)-O because of the small change in $\theta_{O,\,res}$ shown in Figure 4.

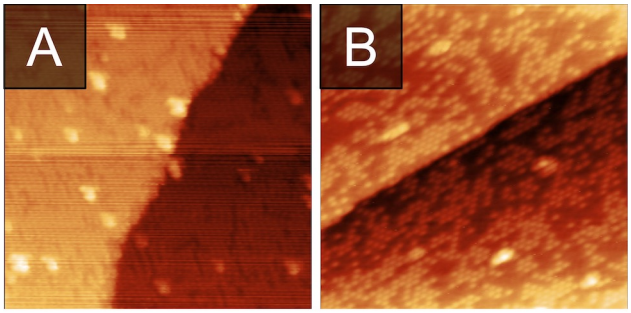

Figure 6: STM image (25 × 25 nm^2) A) of the area around a monatomic Rh(111) step after a 2 L CO exposure to the (2×1)-O adlayer at 220 K, and B) the same sample annealed at 325 K. Imaging conditions were A) 1.08 V and 1.08 nA and B)0.60 V and 487 pA.

Figure 6A shows STM images of the (2×1)-O Rh(111) surface after a 2 L CO exposure at 220 K near a step edge. Looking more closely at the step edges of the surface, the structure of the area around the step was not much different that either the upper or lower terrace (Figure 6A). However, as shown by the STM image in Figure 6B, after annealing to 325 K there was noticeably less (2×2)-2O+CO structure proximal to the step edges. This was interesting because step edges and defect sites are often the most reactive sites on a metal surface, but it has been reported recently, in an electrochemical study, that CO oxidation on the terraces was preferred over step edges [41], and the same was suggested by the STM image in Figure 6B. The fact that there was insufficient thermal energy during the CO exposure for CO_{ad} or O_{ad} to diffuse to lower coordinated sites, where reaction may have been facile, could explain why the CO islands persisted in the STM images in Figures 5 and 6 and the non-regeneration of the low-barrier sites at temperatures of 350 K or less.

Conclusions

The effects of temperature and duration of CO exposures on the oxidation of CO by O_{ad} on Rh(111) were studied. Rh(111) surfaces prepared with the (2×1)-O adlayer were exposed to CO at several temperatures between 100 K and 350 K, and CO exposures

between 5 and 300 L were performed at both 300 K and 350 K. TPD measurements quantified the CO_2 yield between 300 K and 600 K, and $\theta_{O,res}$ after CO oxidation between 600 K and 1400 K. We found that $\theta_{O,\,res}$ was systematically lower after CO exposures at 350 K compared to exposures at 300 K or lower. The CO oxidation rate was greater at 350 K than at 300 K, as observed in the TPD experiments, yet $\theta_{O,res}$ and Y_{CO_2}, did not change as the CO exposure increased. These findings mean that there are multiple reaction pathways available for CO oxidation on Rh(111), and that the lower-barrier pathway involves reaction sites that were not regenerated at temperatures of 350 K or below. The lower-barrier reaction did not occur below 300 K, as indicated by invariant Y_{CO_2} and $\theta_{O,res}$ for exposures CO at temperatures of 300 K or below. These observations show that even for homogeneous surfaces, multiple reaction pathways are accessible for CO oxidation and that complete, accurate models for heterogeneously catalyzed oxidation reactions must include more channels than only reaction between co-adsorbed species.

Acknowledgements

We wish to acknowledge partial support from the National Science Foundation (CHE-1800291). Acknowledgement is made to the Donors of the American Chemical Society Petroleum Research Fund for partial support of this research through Grant PRF #54770-DNI5. This work was also supported by the College of Arts and Sciences at Loyola University Chicago. R. G. Farber thanks The Arthur J. Schmitt Foundation for support during this work. We also want to thank Alex Kandel from Notre Dame for his generous loan of the LEED.

References:

[1] Z. Boukha, M. Gil-Calvo, B. de Rivas, J.R. González-Velasco, J.I. Gutiérrez-Ortiz, R. López-Fonseca, Behaviour of Rh supported on hydroxyapatite catalysts in partial oxidation and steam reforming of methane: On the role of the speciation of the Rh particles, Appl. Catal., A, 556 (2018) 191-203.

[2] B.C. Michael, A. Donazzi, L.D. Schmidt, Effects of H_2O and CO_2 addition in catalytic partial oxidation of methane on Rh, J. Catal., 265 (2009) 117-129.

[3] A.P.E. York, T. Xiao, M.L.H. Green, Brief Overview of the Partial Oxidation of Methane to Synthesis Gas, Top. Catal., 22 (2003) 345-358.

[4] J. Wei, E. Iglesia, Structural requirements and reaction pathways in methane activation and chemical conversion catalyzed by rhodium, J. Catal., 225 (2004) 116-127.

[5] P.A. Thiel, J.T. Yates, W.H. Weinberg, Interaction Of Oxygen With The Rh(111) Surface, Surf. Sci., 82 (1979) 22-44.

[6] C. Zhang, E. Lundgren, P.A. Carlsson, O. Balmes, A. Hellman, L.R. Merte, M. Shipilin, W. Onderwaater, J. Gustafson, Faceting of Rhodium(553) in Realistic Reaction Mixtures of Carbon Monoxide and Oxygen, J. Phys. Chem. C, 119 (2015) 11646-11652.

[7] C.H.F. Peden, D.W. Goodman, D.S. Blair, P.J. Berlowitz, G.B. Fisher, S.H. Oh, Kinetics of Carbon Monoxide Oxidation by Oxygen or Nitric Oxide on Rhodium(111) and Rhodium(100) Single Crystals, J. Phys. Chem., 92 (1988) 1563-1567.

[8] J.N. Wilson, R.A. Pedigo, F. Zaera, Kinetics and Mechanism of Catalytic Partial Oxidation Reactions of Alkanes on Rhodium Surfaces, J. Am. Chem. Soc., 130 (2008) 15796-15797.

[9] K.D. Gibson, D.R. Killelea, S.J. Sibener, Comparison of the Surface and Subsurface Oxygen Reactivity and Dynamics with CO Adsorbed on Rh(111), J. Phys. Chem. C, 118 (2014) 14977-14982.

[10] K.D. Gibson, M. Viste, S.J. Sibener, Applied reaction dynamics: Efficient synthesis gas production via single collision partial oxidation of methane to CO on Rh(111), J. Chem. Phys., 125 (2006) 133401.

[11] R.G. Farber, M.E. Turano, D.R. Killelea, Identification of Surface Sites for Low-Temperature Heterogeneously Catalyzed CO Oxidation on Rh(111), ACS Catal., 8 (2018) 11483-11490.

[12] R.G. Farber, M.E. Turano, E.C.N. Oskorep, N.T. Wands, L.B.F. Juurlink, D.R. Killelea, Exposure of Pt(5 5 3) and Rh(1 1 1) to atomic and molecular oxygen: do defects enhance subsurface oxygen formation?, J. Phys.-Condes. Matt., 29 (2017) 164002.

[13] R.G. Farber, M.E. Turano, E.C.N. Oskorep, N.T. Wands, E.V. Iski, D.R. Killelea, The Quest for Stability: Structural Dependence of Rh(111) on Oxygen Coverage at Elevated Temperature, J. Phys. Chem. C, 121 (2017) 10470-10475.

[14] J. Derouin, R.G. Farber, D.R. Killelea, Combined STM and TPD Study of Rh(111) Under Conditions of High Oxygen Coverage, J. Phys. Chem. C, 119 (2015) 14748-14755.

[15] P. Brault, H. Range, J.P. Toennies, Molecular beam studies of sticking of oxygen on the Rh(111) surface, J. Chem. Phys., 106 (1997) 8876-8889.

[16] H. Xu, K.Y.S. Ng, STM study of oxygen on Rh(111), Surf. Sci., 375 (1997) 161-170.

[17] S. Schwegmann, H. Over, V. DeRenzi, G. Ertl, The atomic geometry of the O and CO+O phases on Rh(111), Surf. Sci., 375 (1997) 91-106.

[18] K.C. Wong, W. Liu, K.A.R. Mitchell, LEED crystallographic analysis for the Rh(111)-(2x1)-O surface structure, Surf. Sci., 360 (1996) 137-143.

[19] K.A. Peterlinz, S.J. Sibener, Absorption, adsorption, and desorption studies of the oxygen/Rh(111) system using O_2, NO, and NO_2, J. Phys. Chem., 99 (1995) 2817-2825.

[20] J. Derouin, R.G. Farber, M.E. Turano, E.V. Iski, D.R. Killelea, Thermally Selective Formation of Subsurface Oxygen in Ag(111) and Consequent Surface Structure, ACS Catal., 6 (2016) 4640-4646.

[21] K.D. Gibson, M. Viste, E. Sanchez, S.J. Sibener, Physical and chemical properties of high density atomic oxygen overlayers under ultrahigh vacuum conditions: (1x1)-O/Rh(111), J. Chem. Phys., 112 (2000) 2470-2478.

[22] K.D. Gibson, M. Viste, E.C. Sanchez, S.J. Sibener, High density adsorbed oxygen on Rh(111) and enhanced routes to metallic oxidation using atomic oxygen, J. Chem. Phys., 110 (1999) 2757-2760.

[23] S. Marchini, C. Sachs, J. Wintterlin, STM investigation of the (2x2)O and (2x1)O structures on Rh(111), Surf. Sci., 592 (2005) 58-64.

[24] R.J. Koestner, M.A. Vanhove, G.A. Somorjai, A surface crystallography study by dynamical LEED of the ($\sqrt{3}$ by $\sqrt{3}$)r30° CO structure on the Rh(111) crystal-surface, Surf. Sci., 107 (1981) 439-458.

[25] L.H. Dubois, G.A. Somorjai, Chemisorption of CO and CO_2 on Rh(111) studied by high-resolution electron-energy loss spectroscopy, Surf. Sci., 91 (1980) 514-532.

[26] M.A. Vanhove, R.J. Koestner, J.C. Frost, G.A. Somorjai, The structure of Rh(111)(2x2)-3CO from LEED intensities - simultaneous bridge and near-top adsorption in a distorted compact hexagonal CO overlayer, Surf. Sci., 129 (1983) 482-506.

[27] P. Cernota, K. Rider, H.A. Yoon, M. Salmeron, G. Somorjai, Dense structures formed by CO on Rh(111) studied by scanning tunneling microscopy, Surf. Sci., 445 (2000) 249-255.

[28] M.J.P. Hopstaken, J.W. Niemantsverdriet, Structure sensitivity in the CO oxidation on rhodium: Effect of adsorbate coverages on oxidation kinetics on Rh(100) and Rh(111), J. Chem. Phys., 113 (2000) 5457-5465.

[29] A.J. Jaworowski, A. Beutler, F. Strisland, R. Nyholm, B. Setlik, D. Heskett, J.N. Andersen, Adsorption sites in O and CO coadsorption phases on Rh(111) investigated by high-resolution core-level photoemission, Surf. Sci., 431 (1999) 33-41.

[30] F. Gao, Y. Cai, K.K. Gath, Y. Wang, M.S. Chen, Q.L. Guo, D.W. Goodman, CO Oxidation on Pt-Group Metals from Ultrahigh Vacuum to Near Atmospheric Pressures. 1. Rhodium, J. Phys. Chem. C, 113 (2009) 182-192.

[31] J.I. Flege, P. Sutter, In situ structural imaging of CO oxidation catalysis on oxidized Rh(111), Phys. Rev. B, 78 (2008) 153402.

[32] E. Lundgren, J. Gustafson, A. Resta, J. Weissenrieder, A. Mikkelsen, J.N. Andersen, L. Kohler, G. Kresse, J. Klikovits, A. Biederman, M. Schmid, P. Varga, The surface oxide as a source of oxygen on Rh(111), J. Electron Spectrosc., 144 (2005) 367-372.

[33] J. Gustafson, O. Balmes, C. Zhang, M. Shipilin, A. Schaefer, B. Hagman, L.R. Merte, N.M. Martin, P.A. Carlsson, M. Jankowski, E.J. Crumlin, E. Lundgren, The Role of Oxides in Catalytic CO Oxidation over Rhodium and Palladium, ACS Catal., 8 (2018) 4438-4445.

[34] R. Westerstrom, O. Balmes, A. Resta, R. van Rijn, J. Gustafson, R. Westerström, X. Torrelles, C.T. Herbschleb, J.W.M. Frenken, E. Lundgren, Catalytic Activity of the Rh Surface Oxide: CO Oxidation over Rh(111) under Realistic Conditions, J. Phys. Chem. C, 114 (2010) 4580-4583.

[35] P. Feulner, D. Menzel, Simple ways to improve ''flash desorption'' measurements from single crystal surfaces, J. Vac. Sci. Technol., 17 (1980) 662-663.

[36] D. Nečas, P. Klapetek, Gwyddion: an open-source software for SPM data analysis, Cent. Eur. J. Phys., 10 (2012) 181-188.

[37] G. Krenn, I. Bako, R. Schennach, CO adsorption and CO and O coadsorption on Rh(111) studied by reflection absorption infrared spectroscopy and density functional theory, J. Chem. Phys., 124 (2006) 144703.

[38] M. Mavrikakis, J. Rempel, J. Greeley, L.B. Hansen, J.K. Norskov, Atomic and molecular adsorption on Rh(111), J. Chem. Phys., 117 (2002) 6737-6744.

[39] E.G. Seebauer, A.C.F. Kong, L.D. Schmidt, Surface diffusion of hydrogen and CO on Rh(111): Laser‐induced thermal desorption studies, J. Chem. Phys., 88 (1988) 6597-6604.

[40] J. Neugebohren, D. Borodin, H.W. Hahn, J. Altschaffel, A. Kandratsenka, D.J. Auerbach, C.T. Campbell, D. Schwarzer, D.J. Harding, A.M. Wodtke, T.N. Kitsopoulos, Velocity-resolved kinetics of site-specific carbon monoxide oxidation on platinum surfaces, Nature, 558 (2018) 280-+.

[41] S.C.S. Lai, N.P. Lebedeva, T.H.M. Housmans, M.T.M. Koper, Mechanisms of Carbon Monoxide and Methanol Oxidation at Single-crystal Electrodes, Top. Catal., 46 (2007) 320-333.